



# Clinical Findings and Optical Coherence Tomography Measurements of Pediatric Patients with Papilledema and Pseudopapilledema

✉ Ayşin Tuba Kaplan\*, ✉ Sibel Öskan Yalçın\*, ✉ Safiye Güneş Sağer\*\*

\*University of Health Sciences Türkiye, Kartal Dr. Lütfi Kırdar City Hospital, Clinic of Ophthalmology, İstanbul, Türkiye  
\*\*University of Health Sciences Türkiye, Kartal Dr. Lütfi Kırdar City Hospital, Clinic of Pediatric Neurology, İstanbul, Türkiye

## Abstract

**Objectives:** To compare the clinical findings and multimodal imaging of pediatric patients diagnosed with papilledema and pseudopapilledema with those of healthy individuals.

**Materials and Methods:** Ninety children (<18 years of age) referred for suspected papilledema were included in this study. All patients underwent optical coherence tomography (OCT) imaging and were compared with normal control subjects.

**Results:** Fifty-eight children diagnosed with pseudopapilledema, 32 children with mild-to-moderate papilledema, and 40 controls were evaluated. The average and all quadrants of retinal nerve fiber layer (RNFL) thickness were significantly higher in the papilledema group than in the pseudopapilledema and control groups ( $p < 0.001$ ). Bruch's membrane opening (BMO) measurements were similar in both groups ( $p > 0.05$ ). The average, nasal, and temporal RNFL thicknesses were significantly higher in the pseudopapilledema group compared with the controls ( $p < 0.001$ ). Area under the receiver operating characteristic (ROC) curve showed high diagnostic ability for RNFL thickness in all quadrants to differentiate papilledema from pseudopapilledema ( $p < 0.001$ ). In the pseudopapilledema group, average, temporal, and inferior RNFL thickness and BMO measurements were significantly higher in eyes with optic nerve head drusen ( $n = 28$ ) compared with those without drusen ( $n = 88$ ) ( $p = 0.035$ ,  $p = 0.022$ ,  $p = 0.040$  and,  $p = 0.047$  respectively).

**Conclusion:** Papilledema and pseudopapilledema show great differences in evaluation, follow-up, and prognosis. Using non-invasive methods such as newly developed OCT techniques in differential diagnosis can relieve patients with pseudopapilledema from the stress and financial burden of expensive, extensive, and invasive procedures.

**Keywords:** Optic nerve, drusen, papilledema, optical coherence tomography, tilted disc

**Cite this article as:** Kaplan AT, Öskan Yalçın S, Sağer SG. Clinical Findings and Optical Coherence Tomography Measurements of Pediatric Patients with Papilledema and Pseudopapilledema. *Turk J Ophthalmol* 2023;53:294-300

Address for Correspondence: Ayşin Tuba Kaplan, University of Health Sciences Türkiye, Kartal Dr. Lütfi Kırdar City Hospital, Clinic of Ophthalmology, İstanbul, Türkiye

E-mail: aysintuba@yahoo.com ORCID-ID: orcid.org/0000-0003-0793-5530

Received: 17.09.2022 Accepted: 15.02.2023

DOI: 10.4274/tjo.galenos.2023.81504

## Introduction

Optic nerve head edema due to increased intracranial pressure is called papilledema. Pseudopapilledema is not true edema but is defined by the presence of blurring and swelling at the borders of the optic nerve head due to structural anomalies.<sup>1</sup> Especially in children, distinguishing the two diagnoses is vital. Misdiagnosis of papilledema as pseudopapilledema can be life-threatening, and conversely, diagnosis of pseudopapilledema as papilledema can lead to unnecessary, invasive, and expensive procedures and treatments.<sup>1,2</sup>

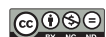
The prevalence of optic nerve head drusen (ONHD) is approximately 0.4% in children and 2.4% in adults. This difference is probably due to the smaller and deeper location of drusen in children.<sup>3,4,5,6</sup> High hypermetropia, crowded or congenitally anomalous optic nerves, and tilted optic discs may also cause a pseudopapilledema appearance in children.<sup>7,8</sup>

To diagnose true papilledema, neuroimaging (computed tomography [CT], magnetic resonance imaging [MRI]) and invasive procedures (lumbar puncture [LP]) are required. Performing these tests in children is not easy and may require sedation or general anesthesia. Non-invasive imaging modalities such as ocular ultrasonography (USG), fundus autofluorescence (FAF), and optical coherence tomography (OCT) can help diagnose true and pseudopapilledema.

The purpose of this study was to present the clinical data of our pediatric patients who were diagnosed as having pseudopapilledema or papilledema and to compare their OCT findings with healthy subjects.

## Materials and Methods

Patients under 18 years of age who were diagnosed as having pseudopapilledema or mild papilledema and had at least 1 year of follow-up between 2018 and 2020 were included in the study. This study was approved by the Ethics Committee of University



of Health Sciences Türkiye, Kartal Dr. Lütfi Kırdar Şehir Hospital (decision no: 2022/514/236/15, date: 26.10.2022). All procedures and data collection were conducted in accordance with the Declaration of Helsinki. The children were referred to a tertiary hospital by pediatric neurologists for evaluation of suspected papilledema or by an ophthalmologist because of disc margin blurring detected in routine examinations.

One hundred sixteen eyes of 58 children in the pseudopapilledema group and 64 eyes of 32 children in the papilledema group were included in this retrospective study. Eighty eyes of 40 patients of similar age and sex were included as the control group. The participants in the control group had normal healthy eyes and had no visual field or retinal nerve fiber layer (RNFL) defects.

In patients with suspected papilledema on ophthalmologic examination, the presence of headache with characteristics indicating increased intracranial pressure and accompanying symptoms such as diplopia, vomiting, and visual symptoms are guides for further investigation. In such cases, our primary approach is to perform a neurologic examination and MRI. If there is no mass or other pathology that might cause papilledema on MRI, LP is performed. The presence of possible signs of high intracranial pressure (empty sella, flattening of the posterior globe, tortuosity of the optic nerve or increase in perioptic cerebrospinal fluid) on MRI strengthens the diagnosis of papilledema in the presence of suspicious optic disc appearance or certain symptoms.<sup>2</sup> Otherwise, if there is no sign of increased intracranial pressure on MRI or patients have no specific symptoms, patients are directed to advanced ophthalmologic examinations for the diagnosis of pseudopapilledema. These patients are followed up regularly for at least 6 months.

In cases of suspected pseudopapilledema, B-scan USG, FAF, fluorescein angiography (FA), and spectral domain (SD)-OCT scans were performed. The ocular examination included examinations of visual acuity, color vision (Ishihara color plate), light reflex, ocular motility, visual fields (Humphrey 30-2; Allergan, Irvine, CA, USA), anterior segment, and fundus. Optic nerve head swelling was graded according to the Frisen scale.<sup>9</sup> Grade III-IV papilledema patients were excluded from the study. Fundus images of all patients were obtained from the first examination to monitor changes. ONHD was defined as hyperechoic and posterior acoustic shadowing structures within or on the optic nerve surface on B-scan (E-Z Scan AB5500+; Sonomed, Lake Success, NY, USA), autofluorescence in the optic nerve on FAF imaging (Canon CX-1; Canon Inc., Tokyo, Japan), absence of dye leakage in FA (Canon CX-1; Canon Inc, Tokyo, Japan), or a hyporeflexive core surrounded by hyperreflective margins on SD-OCT (Nidek RS-3000 Advance; Nidek Co., Aichi, Japan).<sup>10</sup> Enlargement of the optic nerve sheath with a hypoechogenic crescent sign surrounding the optic nerve, which may suggest papilledema, was assessed and measurements were made using A-scans in necessary cases.<sup>11</sup> Peripapillary hyperreflective ovoid mass-like structures (PHOMS) were defined as hyperreflective structures surrounding the optic nerve and were located subretinally above Bruch's membrane on OCT.<sup>12,13</sup>

The diagnosis of pseudopapilledema was defined as the presence of spontaneous venous pulsation and normal MRI, venography, or LP without specific symptoms evaluated by a pediatric neurologist, and stability of the optic nerve head on examination and imaging in at least three follow-up visits at 6-month intervals. After 1 year of follow-up, optic nerve appearances were stable and no change was observed in the diagnosis of our patients with pseudopapilledema.

The peripapillary RNFL thickness in all four quadrants, average RNFL thickness, and Bruch's membrane opening (BMO) were measured using SD-OCT. The RNFL thickness in each 90-degree quadrant (superior, inferior, temporal, and nasal) was calculated within a 3.45-mm diameter scan circle around the optic disc. The BMO was defined as the horizontal transverse diameter of the neural canal opening (in micrometers) at the level of the retinal pigment epithelium and Bruch's membrane.<sup>14</sup> BMO measurements were performed manually using the OCT software. The quality of all scans was evaluated and scans were excluded if they had artifacts or errors. Particular attention was paid to patients with high myopia (>6.0 diopters) and hyperopia (>6.0 diopters). In such patients, the errors that might arise from disc centration were noted and images with signal strength >5 were evaluated. Optic nerve examinations and images were evaluated by two experienced ophthalmologists, and SD-OCT measurements were analyzed by the same experienced technician.

#### Statistical Analysis

The data were evaluated in the IBM SPSS Statistics Standard Concurrent User V 26 (IBM Corp., Armonk, New York, USA) statistical package program. Descriptive statistics were given as the number of units (n), percentage (%), mean and standard deviation (mean  $\pm$  SD), median (M), and interquartile range (IQR). The normal distribution of the data of numerical variables was evaluated using the Shapiro-Wilk test of normality. Homogeneity of variances was evaluated using Levene's test. The ages of the patients in the groups were compared using One-way analysis of variance (ANOVA), and Pearson's chi-square test was used for sex comparisons. Since the right and left eyes of the patients were evaluated together, comparisons between groups for OCT variables were made using linear mixed model analysis. Bonferroni correction was applied for multiple comparisons. A value of  $p < 0.05$  was considered statistically significant.

#### Results

The study included 116 eyes of 58 patients with pseudopapilledema, 64 eyes of 32 patients with mild-to-moderate papilledema, and 80 eyes of 40 healthy normal individuals. The mean ages of the children were  $13.2 \pm 3.2$  years in the pseudopapilledema group,  $12.1 \pm 2.8$  years in the papilledema group, and  $12.0 \pm 3.3$  years in the control group. The age and sex distributions of the groups were statistically similar (Table 1).

Of the 58 children in the pseudopapilledema group, 30 (52%) presented with headaches, 8 (14%) with blurred vision, and 20 (34%) children were completely asymptomatic and referred for

examination of the optic disc. In the papilledema group, the most common symptom was headache (50%) with visual symptoms, followed by double vision (21.8%), tinnitus (15.6%), and transient vision loss (12.5%). The etiologies of papilledema were idiopathic intracranial hypertension (IIH) (n=24, 75%), cerebral venous sinus thrombosis (n=5, 15.6%), and intracranial tumor (n=3, 9.4%). The mean visual acuity was  $0.05 \pm 0.04$  logarithm of the minimum angle of resolution (logMAR) in the pseudopapilledema group,  $0.02 \pm 0.04$  logMAR in the papilledema group, and  $0.05 \pm 0.1$  logMAR in the control group.

Of the patients diagnosed as having pseudopapilledema, 44 (76%) underwent MRI, 2 (3.4%) underwent CT, and 30 (52%) underwent LP. The mean opening pressure was  $21.5 \pm 3.07$  (range, 14-25) cm H<sub>2</sub>O. Three children diagnosed as having pseudopapilledema were using acetazolamide for the misdiagnosis of IIH. The drug was discontinued when the diagnosis was revised. In a patient with optic disc drusen, IIH was also detected and treatment was initiated. Of the 116 eyes with pseudopapilledema, PHOMS were detected in 82 eyes (70.7%), ONHD in 28 eyes (24.1%), crowded discs in 25 eyes (21.6%), and tilted/torsioned discs in 13 eyes (11.2%). Only 2 eyes (7%) had visible ONHD and 26 eyes had buried ONHD (93%). The diagnosis of ONHD was confirmed using USG

in 26 eyes, SD-OCT in 21 eyes, FAF in 11 eyes, and clinical examination in 2 eyes (Figure 1a, b, c). FA was used in 8 patients to diagnose pseudopapilledema.

In the papilledema group, grade 1 papilledema was detected in 19 (29.7%) eyes and grade 2 papilledema was detected in 45 (70.3%) eyes. PHOMS were also detected in 20 (31.2%) of these eyes (Figure 1c). MRI and LP were performed in all patients in the papilledema group. The mean opening pressure was  $37.5 \pm 9.3$  (range, 25-60) cm H<sub>2</sub>O. Patients diagnosed as having papilledema were treated by pediatric neurology or neurosurgery and followed up ophthalmologically.

Table 2 gives the RNFL thickness and BMO measurements in both groups. The average and all quadrants of RNFL thickness were significantly higher in the papilledema group than in the pseudopapilledema and control groups ( $p < 0.001$ ). The BMO measurements were similar in both groups ( $p > 0.05$ ). The average, nasal, and temporal RNFL thicknesses were significantly higher in the pseudopapilledema group compared with the controls ( $p < 0.001$ ). Within the pseudopapilledema group, average, temporal, and inferior RNFL thickness and BMO measurements were significantly higher in eyes with ONHD compared to those without ONHD ( $p = 0.035$ ,  $p = 0.022$ ,  $p = 0.040$ , and  $p = 0.047$ , respectively) (Table 3).

	<b>Papilledema (n=32)</b>	<b>Pseudopapilledema (n=58)</b>	<b>Control (n=40)</b>	<b>p value</b>
<b>Sex, n (%)</b>				
Boy/girl	8 (25.0)/24 (75.0)	20 (34.5)/38 (65.5)	14 (35.0)/26 (65.0)	0.632*
<b>Age, years mean ± SD</b>	12.1 ± 2.8	13.2 ± 3.2	12.0 ± 3.3	
Median (min-max)	12 (6-16)	13 (5-18)	12 (7-18)	0.106**

\*Pearson chi-square test, \*\*One-way analysis of variance, SD: Standard deviation

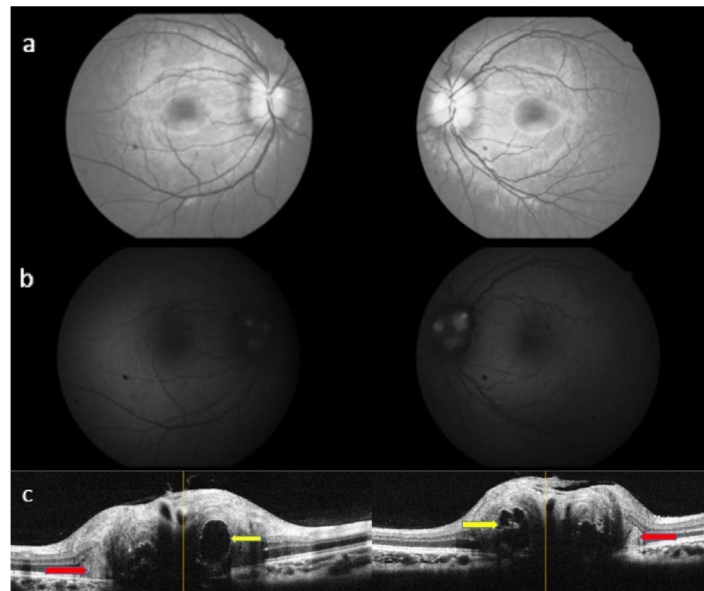


**Figure 1.** (a) Fundus red-free photo of a patient with visible optic nerve head drusen (ONHD); (b) fundus autofluorescence image of ONHD; (c) optical coherence tomography image of ONHD (yellow arrow) and peripapillary hyperreflective ovoid mass-like structures (red arrow) in the same patient

Table 4 gives the results of ROC analyses of RNFL thickness and BMO in differentiating papilledema from pseudopapilledema. Average RNFL thickness had the highest area under the curve (AUC), followed by temporal, nasal, superior, and inferior RNFL thickness. BMO had a smaller AUC, with a cutoff point of 1563  $\mu\text{m}$  resulting in a sensitivity and specificity of 75% and 52.6%, respectively.

## Discussion

In recent years, children's referrals to ophthalmology departments have increased due to suspected papilledema. Making the correct diagnosis is a difficult and stressful process for both the physician and patient. The misdiagnosis rate of papilledema in childhood has been reported as up to 76%.<sup>15</sup>

Most of these children undergo unnecessary MRI, CT, or other imaging and several LPs.

Headache that occurs due to IIH increases especially in the morning and when lying down, and is sometimes associated with neck and shoulder pain due to stretching of the dural sheaths of spinal roots. Questioning the character of the headache and examining for accompanying additional symptoms such as transient visual obscurations, double vision, vomiting, and tinnitus are necessary for a detailed history and differential diagnosis. Headache was more common and was a non-specific symptom in most of the children in our study; however, MRI was performed in 76% of these children and LP was performed in 52%. Liu et al.<sup>16</sup> reported that children with pseudopapilledema referred for suspected papilledema over a

**Table 2. Comparison of optical coherence tomography parameters by group**

	Groups			Pairwise comparisons*		
	Papilledema (n=64 eyes) Mean $\pm$ SEM	Pseudopapilledema (n=116 eyes) Mean $\pm$ SEM	Control (n=80 eyes) Mean $\pm$ SEM	Papilledema vs. pseudopapilledema	Papilledema vs. control	Pseudopapilledema vs. control
RNFL	140.4 $\pm$ 2.3	117.2 $\pm$ 1.7	106.7 $\pm$ 2.1	<0.001	<0.001	<0.001
Nasal RNFL	117.3 $\pm$ 2.6	98.5 $\pm$ 1.9	72.5 $\pm$ 2.4	<0.001	<0.001	<0.001
Temporal RNFL	106.6 $\pm$ 2.2	84.6 $\pm$ 1.6	74.5 $\pm$ 1.9	<0.001	<0.001	<0.001
Superior RNFL	161.7 $\pm$ 3.5	137.8 $\pm$ 3.6	136.7 $\pm$ 3.3	<0.001	<0.001	0.999
Inferior RNFL	161.0 $\pm$ 3.9	146.1 $\pm$ 2.9	140.0 $\pm$ 3.6	0.009	<0.001	0.559
BMO	1660.6 $\pm$ 23.4	1596.1 $\pm$ 17.3	1591.8 $\pm$ 21.2	0.086	0.094	0.999

\*Significant values based on linear mixed model, RNFL: Retinal nerve fiber layer, BMO: Bruch's membrane opening, SEM: Standard error of the mean

**Table 3. Comparison of optical coherence tomography parameters according to the presence of drusen in the pseudopapilledema group**

	No drusen (n=88) Mean $\pm$ SEM	Drusen (n=28) Mean $\pm$ SEM	p value*
Average RNFL	114.8 $\pm$ 2.23	124.4 $\pm$ 3.8	0.035
Nasal RNFL	97.1 $\pm$ 2.3	102.3 $\pm$ 4.0	0.260
Temporal RNFL	82.3 $\pm$ 1.9	91.1 $\pm$ 3.2	0.022
Superior RNFL	134.9 $\pm$ 3.4	145.5 $\pm$ 5.9	0.128
Inferior RNFL	141.8 $\pm$ 4.2	159.4 $\pm$ 7.2	0.040
BMO	1575.2 $\pm$ 20.8	1658.8 $\pm$ 35.4	0.047

\*Significant values based on linear mixed model, RNFL: Retinal nerve fiber layer, BMO: Bruch's membrane opening, SEM: Standard error of the mean

**Table 4. Results of receiver operating characteristic curve analysis of optical coherence tomography parameters in papilledema vs. pseudopapilledema**

	Cut-off	AUC	95% CI	p value	Sens	Spec	PPV	NPV
Average RNFL	>125	0.868	0.809-0.914	<0.001	90.6	76.7	68.2	93.7
Nasal RNFL	>100	0.819	0.755-0.873	<0.001	82.8	75.9	65.4	88.9
Temporal RNFL	>96	0.862	0.802-0.908	<0.001	82.8	83.6	73.6	89.8
Superior RNFL	>137	0.797	0.731-0.853	<0.001	95.3	58.6	56.0	95.8
Inferior RNFL	>144	0.719	0.647-0.783	<0.001	82.8	56.0	51.0	85.5
BMO	>1563	0.632	0.557-0.703	0.002	75.0	52.6	46.6	79.2

RNFL: Retinal nerve fiber layer, BMO: Bruch's membrane opening, AUC: Area under the curve, CI: Confidence interval, Sens: Sensitivity, Spec: Specificity, PPV: Positive predictive value, NPV: Negative predictive value

6-year period underwent LP, MRI, and CT at rates of 53.8%, 73.1%, and 34.6%, respectively. They suggested that detailed histories and expert ophthalmologic examinations in the early period would prevent unnecessary tests and treatments.

It is very difficult to distinguish papilledema from pseudopapilledema in childhood. For instance, ONHD, the most common cause of pseudopapilledema, is buried deeper in children and mimics papilledema. Over time, it becomes more superficial and is easier to detect.<sup>17</sup> In addition, because ONHD is less calcified in children than in adults, it is difficult to diagnose it with USG, which is one of the traditional diagnostic methods.<sup>18</sup> Similarly, ONHD may not be detected with FAF and FA because it is hidden deep within the neural tissue.<sup>17,18,19</sup>

Although pseudopapilledema was diagnosed in 116 eyes in our study, we detected ONHD in only 28 eyes. In all of these patients, USG confirmed the diagnosis, and OCT helped in 21 eyes. It was not possible to detect buried and non-calcified drusen because the mean age of our patients was young ( $13.2 \pm 3.2$  years). Previously, USG was considered the gold standard for diagnosing ONHD. However, ONHD is now more reliably diagnosed using enhanced depth imaging (EDI) OCT, which enables high-resolution visualization of the optic nerve head. In the pediatric population, this advantage is limited with increasing depth. Deeper ONHD has a lower resolution, often resulting in a poorer demarcation of their posterior borders.<sup>20,21</sup> Sim et al.<sup>22</sup> compared EDI-OCT, non-EDI-OCT, and FAF imaging in 28 children with definite ONHD confirmed using USG and determined that the three modalities revealed ONHD in 24, 21, and 18 eyes, respectively. In that study, EDI-OCT was not as successful as USG in detecting ONHD, unlike in adults. Similarly, the authors attributed this to a high incidence of buried ONHD in children.<sup>22</sup>

In our study, RNFL average and all quadrant thickness values were significantly higher in the papilledema group than in the pseudopapilledema and control groups ( $p < 0.001$ ) and the average, temporal, and inferior RNFL thickness values were significantly higher in the pseudopapilledema group with ONHD compared to those without ONHD ( $p = 0.035$ ,  $p = 0.022$ , and  $p = 0.040$ , respectively). Although OCT studies comparing papilledema and pseudopapilledema have been performed in recent years, no absolute values have been shown to be diagnostic for papilledema. In studies using SD-OCT, Lee et al.<sup>23</sup> reported significantly greater RNFL thickness in patients with papilledema than in patients with ONHD ( $174.1 \pm 53.5$   $\mu\text{m}$  vs.  $119.2 \pm 20.2$   $\mu\text{m}$ ), as well as higher average and temporal RNFL thickness in patients with pseudopapilledema compared to the control group. Aghsaei Fard et al.<sup>24</sup> determined that the average and all sectoral peripapillary RNFL thicknesses were higher in the papilledema group than in the other groups, and they reported an AUC of 0.82 for the ability of peripapillary RNFL to distinguish papilledema from pseudopapilledema. Swanson et al.<sup>25</sup> reported 79% sensitivity and 81% specificity in determining increased intracranial pressure due to craniosynostosis when the RNFL cut-off value was accepted as 208  $\mu\text{m}$ . It is noteworthy that the cut-off value was quite high for mild and moderate

papilledema. In our study the average RNLF had the highest AUC (0.868) with a cut-off value of 125  $\mu\text{m}$  in papilledema compared to pseudopapilledema. Kulkarni et al.<sup>26</sup> found no significant difference between Frisen grade 2 mild papilledema and ONHD in terms of RNFL thickness. Chang et al.<sup>27</sup> was unable to make an accurate classification due to the overlap of RNFL thickness values in papilledema (mean: 142  $\mu\text{m}$ , range: 91-199  $\mu\text{m}$ ) and ONHD (mean: 125  $\mu\text{m}$ , range: 98-162  $\mu\text{m}$ ). In patients with pseudopapilledema, an increase in thickness has been demonstrated in different quadrants, which is not always consistent with healthy subjects and patients with mild papilledema. It has been suggested that the nasal quadrant in particular can provide important information in the differential diagnosis, and the nasal quadrant values seen in ONHD may be thinner.<sup>23,28,29,30</sup> This hypothesis is explained by the fact that the drusen are mostly located in the nasal quadrant, causing displacement and thinning of the nerve fibers over time. It has also been reported that there is a gradual enhancement in drusen size with age and the optic nerve size is smaller in children than in adults.<sup>4,22,31</sup> In line with previous studies, it was not possible to detect nasal RNFL thinning in children in the early period.<sup>32</sup>

Studies based on optic nerve imaging and OCT suggested that pseudopapilledema might originate from a narrow scleral canal and there could be stasis in the axoplasmic flow due to compression of the peripapillary nerves.<sup>24,33,34</sup> In some studies, as in our study, BMO was similar in the pseudopapilledema, mild papilledema, and control groups.<sup>8,24</sup> Thompson et al.<sup>35</sup> compared BMO in children with mild papilledema and pseudopapilledema and reported a larger mean BMO in the papilledema group than in the pseudopapilledema group and no significant difference between the pseudopapilledema and control groups. However, after the treatment of papilledema, the patients' mean BMO no longer differed significantly from the other groups. It has also been reported that BMO may enlarge in papilledema, non-arteritic ischemic optic neuropathy (NAION), or ONHD, and also shrink again after resolving the edema in the optic nerve.<sup>35,36,37</sup> García-Montesinos et al.<sup>37</sup> reported BMO enlargement in papilledema and NAION. They suggested that during optic nerve swelling, axonal fibers increased in volume and expanded the optic canal, then shrank again when the edema decreased. In another study using time-domain-OCT, it was reported that patients with ONHD and their first-degree relatives did not have narrow scleral canals, and both groups had a larger scleral canal area than the controls.<sup>24</sup> Similarly, Floyd et al.<sup>38</sup> studied 25 patients with ONHD and found larger scleral canals than in 17 control patients. In contrast, Malmqvist et al.<sup>12</sup> reported in their prospective study that children with ONHD had smaller scleral canals than those with normal optic nerves. In our study, BMO was similar in both groups but was higher in pseudopapilledema patients with ONHD than in those without ONHD, and the sensitivity and specificity of BMO in the differentiation of papilledema and pseudopapilledema were quite low. In light of similar studies, we thought that drusen may cause enlargement of the scleral canal over time, depending on their size and location. Significant differences in BMO

measurements between healthy individuals and patients with different optic nerve pathologies suggest that the clinical value of this OCT finding may be limited.

In recent years, the Optic Disc Drusen Studies Consortium has defined an optic nerve head lesion distinct from ONHD.<sup>12</sup> Formerly described as drusen-like or drusen precursors, they are now called PHOMS.<sup>39,40,41,42</sup> It is suggested that the presence of these structures should not be included as a diagnostic criterion for ONHD. Apart from drusen, it can be seen in various forms of optic disc edema and optic disc anomalies.<sup>12,43,44</sup> PHOMS was defined as the OCT finding corresponding to lateral herniation of retinal nerve fibers at the level of Bruch's membrane. They have the appearance of typical hyperreflective lesions surrounding the optic disc in the subretinal area but are neither hyperechogenic structures in B-scan images nor hyperautofluorescent on FAF images.<sup>45</sup>

In our study, PHOMS were detected using SD-OCT in 70.7% of eyes with pseudopapilledema and in 31.2% eyes with papilledema. Mezaad-Koursh et al.<sup>13</sup> emphasized that PHOMS were the most common causes of pseudopapilledema in children and they characterized PHOMS in EDI-OCT, USG, FAF, and infrared images. They reported significant differences between PHOMS and ONHD, as in the study of Teixeira et al.<sup>45</sup> PHOMS are a new structure defined in the optic nerve head, and their development over the years is not clear. Malmqvist et al.<sup>44</sup> studied 5-year changes in children with ONHD and found that crowded disc and axonal distension resulting from the enlargement of optic nerve drusen were associated with PHOMS. It is important to follow up PHOMS because there are insufficient prospective studies about its change and progression, especially in children.

#### Study Limitations

Our study had some limitations. The number of patients was small and it was a retrospective study. Prospective studies with large series are needed to determine the gold standard methods in the differentiation of papilledema and pseudopapilledema in children.

#### Conclusion

In conclusion, a detailed history, complete ophthalmologic examination, and neurologic assessment can provide accurate diagnosis of papilledema or pseudopapilledema in most patients without invasive and expensive procedures. EDI-OCT appears to be an advanced technique with the potential to become the gold standard for identifying and monitoring PHOMS and ONHD in early childhood.

#### Ethics

**Ethics Committee Approval:** This study was approved by the Ethics Committee of University of Health Sciences Türkiye, Kartal Dr. Lütfi Kırdar Şehir Hospital (decision no: 2022/514/236/15, date: 26.10.2022).

**Informed Consent:** Obtained.

**Peer-review:** Externally peer-reviewed.

#### Authorship Contributions

Surgical and Medical Practices: A.T.K., S.Ö.Y., S.G.S., Concept: A.T.K., S.G.S., Design: A.T.K., Data Collection or

Processing: A.T.K., S.Ö.Y., S.G.S., Analysis or Interpretation: A.T.K., S.Ö.Y., Literature Search: A.T.K., S.Ö.Y., Writing: A.T.K.

**Conflict of Interest:** No conflict of interest was declared by the authors.

**Financial Disclosure:** The authors declared that this study received no financial support.

#### References

- Leon M, Hutchinson AK, Lenhart PD, Lambert SR. The cost-effectiveness of different strategies to evaluate optic disk drusen in children. *J AAPOS*. 2014;18:449-452.
- Mishra A, Mordekar SR, Rennie IG, Baxter PS. False diagnosis of papilloedema and idiopathic intracranial hypertension. *Eur J Paediatr Neurol*. 2007;11:39-42.
- Erkkila H. Clinical appearance of optic disc drusen in childhood. *Albrecht Von Graefes Arch Klin Exp Ophthalmol*. 1975;193:1-18.
- Auw-Haedrich C, Staubach F, Witschel H. Optic disk drusen. *Surv Ophthalmol*. 2002;47:515-532.
- Frisén L. Evolution of drusen of the optic nerve head over 23 years. *Acta Ophthalmol*. 2008;86:111-112.
- Spencer TS, Katz BJ, Weber SW, Digre KB. Progression from anomalous optic discs to visible optic disc drusen. *J Neuroophthalmol*. 2004;24:297-298.
- Davis PL, Jay WM. Optic nerve head drusen. *Semin Ophthalmol*. 2003;18:222-242.
- Lam BL, Morais CG Jr, Pasol J. Drusen of the optic disc. *Curr Neurol Neurosci Rep*. 2008;8:404-408.
- Frisén L. Swelling of the optic nerve head: a staging scheme. *J Neurol Neurosurg Psychiatry*. 1982;45:13-18.
- Rebolleda G, Kawasaki A, de Juan V, Oblanca N, Muñoz-Negrete FJ. Optical Coherence Tomography to Differentiate Papilledema from Pseudopapilledema. *Curr Neurol Neurosci Rep*. 2017;17:74.
- Neudorfer M, Ben-Haim MS, Leibovitch I, Kesler A. The efficacy of optic nerve ultrasonography for differentiating papilloedema from pseudopapilloedema in eyes with swollen optic discs. *Acta Ophthalmol*. 2013;91:376-380.
- Malmqvist L, Bursztyn L, Costello F, Digre K, Fraser JA, Fraser C, Katz B, Lawlor M, Petzold A, Sibony P, Warner J, Wegener M, Wong S, Hamann S. The Optic Disc Drusen Studies Consortium Recommendations for Diagnosis of Optic Disc Drusen Using Optical Coherence Tomography. *J Neuroophthalmol*. 2018;38:299-307.
- Mezaad-Koursh D, Klein A, Rosenblatt A, Teper Roth S, Neudorfer M, Loewenstein A, Igllicki M, Zur D. Peripapillary hyperreflective ovoid mass-like structures—a novel entity as frequent cause of pseudopapilloedema in children. *Eye (Lond)*. 2021;35:1228-1234.
- Anand A, Pass A, Urfy MZ, Tang R, Cajavilca C, Calvillo E, Suarez JJ, Venkatasubba Rao CP, Bershah EM. Optical coherence tomography of the optic nerve head detects acute changes in intracranial pressure. *J Clin Neurosci*. 2016;29:73-76.
- Kovarik JJ, Doshi PN, Collinge JE, Plager DA. Outcome of pediatric patients referred for papilledema. *J AAPOS*. 2015;19:344-348.
- Liu B, Murphy RK, Mercer D, Tychsens L, Smyth MD. Pseudopapilledema and association with idiopathic intracranial hypertension. *Childs Nerv Syst*. 2014;30:1197-1200.
- Chang MY, Pineles SL. Optic disk drusen in children. *Surv Ophthalmol*. 2016;61:745-758.
- Kurz-Levin MM, Landau K. A comparison of imaging techniques for diagnosing drusen of the optic nerve head. *Arch Ophthalmol*. 1999;117:1045-1049.
- Pineles SL, Arnold AC. Fluorescein angiographic identification of optic disc drusen with and without optic disc edema. *J Neuroophthalmol*. 2012;32:17-22.

20. Yi K, Mujat M, Sun W, Burnes D, Latina MA, Lin DT, Deschler DG, Rubin PA, Park BH, de Boer JF, Chen TC. Imaging of optic nerve head drusen: improvements with spectral domain optical coherence tomography. *J Glaucoma*. 2009;18:373-378.
21. Wester ST, Fantès FE, Lam BL, Anderson DR, McSoley JJ, Knighton RW. Characteristics of optic nerve head drusen on optical coherence tomography images. *Ophthalmic Surg Lasers Imaging*. 2010;41:83-90.
22. Sim PY, Soomro H, Karampelas M, Barampouti F. Enhanced Depth Imaging Optical Coherence Tomography of Optic Nerve Head Drusen in Children. *J Neuroophthalmol*. 2020;40:498-503.
23. Lee KM, Woo SJ, Hwang JM. Differentiation of optic nerve head drusen and optic disc edema with spectral-domain optical coherence tomography. *Ophthalmology*. 2011;118:971-977.
24. Aghsaei Fard M, Okhravi S, Moghimi S, Subramanian PS. Optic Nerve Head and Macular Optical Coherence Tomography Measurements in Papilledema Compared With Pseudopapilledema. *J Neuroophthalmol*. 2019;39:28-34.
25. Swanson JW, Xu W, Ying GS, Pan W, Lang SS, Heuer GG, Bartlett SP, Taylor JA. Intracranial pressure patterns in children with craniosynostosis utilizing optical coherence tomography. *Childs Nerv Syst*. 2020;36:535-544.
26. Kulkarni KM, Pasol J, Rosa PR, Lam BL. Differentiating mild papilledema and buried optic nerve head drusen using spectral domain optical coherence tomography. *Ophthalmology*. 2014;121:959-963.
27. Chang MY, Velez FG, Demer JL, Bonelli L, Quiros PA, Arnold AC, Sadun AA, Pineles SL. Accuracy of Diagnostic Imaging Modalities for Classifying Pediatric Eyes as Papilledema Versus Pseudopapilledema. *Ophthalmology*. 2017;124:1839-1848.
28. Johnson LN, Diehl ML, Hamm CW, Sommerville DN, Petroski GF. Differentiating optic disc edema from optic nerve head drusen on optical coherence tomography. *Arch Ophthalmol*. 2009;127:45-49.
29. Sarac O, Tasci YY, Gurdal C, Can I. Differentiation of optic disc edema from optic nerve head drusen with spectral-domain optical coherence tomography. *J Neuroophthalmol*. 2012;32:207-211.
30. Capo H. Don't Miss This! Red Flags in the Pediatric Eye Exam: Blurred Disc Margins. *J Binocul Vis Ocul Motil*. 2019;69:110-115.
31. Sato T, Mrejen S, Spaide RF. Multimodal imaging of optic disc drusen. *Am J Ophthalmol*. 2013;156:275-282.
32. Loo KG, Lim SA, Lim IL, Chan DW. Guiding follow-up of paediatric idiopathic intracranial hypertension with optical coherence tomography. *BMJ Case Rep*. 2016;2016:bcr2015213070.
33. Mullie MA, Sanders MD. Scleral canal size and optic nerve head drusen. *Am J Ophthalmol*. 1985;99:356-359.
34. Jonas JB, Gusek GC, Guggenmoos-Holzmann I, Naumann GO. Pseudopapilledema associated with abnormally small optic discs. *Acta Ophthalmol (Copenh)*. 1988;66:190-193.
35. Thompson AC, Bhatti MT, El-Dairi MA. Bruch's membrane opening on optical coherence tomography in pediatric papilledema and pseudopapilledema. *J AAPOS*. 2018;22:38-43.
36. Rebolleda G, García-Montesinos J, De Dompablo E, Oblanca N, Muñoz-Negrete FJ, González-López JJ. Bruch's membrane opening changes and lamina cribrosa displacement in non-arteritic anterior ischaemic optic neuropathy. *Br J Ophthalmol*. 2017;101:143-149.
37. García-Montesinos J, Muñoz-Negrete FJ, de Juan V, Rebolleda G. Relationship between lamina cribrosa displacement and trans-laminar pressure difference in papilledema. *Graefes Arch Clin Exp Ophthalmol*. 2017;255:1237-1243.
38. Floyd MS, Katz BJ, Digre KB. Measurement of the scleral canal using optical coherence tomography in patients with optic nerve drusen. *Am J Ophthalmol*. 2005;139:664-669.
39. Sarkies NJ, Sanders MD. Optic disc drusen and episodic visual loss. *Brit J Ophthalmol*. 1987;71:537-539.
40. Savino PJ, Glaser JS, Rosenberg MA. A clinical analysis of pseudopapilledema. II. Visual field defects. *Arch Ophthalmol*. 1979;97:71-75.
41. Savino PJ, Guy JR, Trobe JD, McCrary JA, Smith CH, Chrousos GA, Thompson HS, Katz BJ, Brodsky MC, Goodwin JA, Atwell CW, and the Optic Neuritis Study Group. A randomized, controlled trial of corticosteroids in the treatment of acute optic neuritis. *N Engl J Med*. 1992;326:581-588.
42. Horwitz H, Friis T, Modvig S, Roed H, Tsakiri A, Laursen B, Frederiksen JL. Differential diagnoses to MS: experiences from an optic neuritis clinic. *J Neurol*. 2014;261:98-105.
43. Malmqvist L, Bursztyn L, Costello F, Digre K, Fraser JA, Fraser C, Katz B, Lawlor M, Petzold A, Sibony P, Warner J, Wegener M, Wong S, Hamann S. Peripapillary Hyperreflective Ovoid Mass-Like Structures: Is It Optic Disc Drusen or Not?: Response. *J Neuroophthalmol*. 2018;38:568-570.
44. Malmqvist L, Li XQ, Hansen MH, Thomsen AK, Skovgaard AM, Olsen EM, Larsen M, Munch IC, Hamann S. Progression Over 5 Years of Prelaminar Hyperreflective Lines to Optic Disc Drusen in the Copenhagen Child Cohort 2000 Eye Study. *J Neuroophthalmol*. 2020;40:315-321.
45. Teixeira FJ, Marques RE, Mano SS, Couceiro R, Pinto F. Optic disc drusen in children: morphologic features using EDI-OCT. *Eye (Lond)*. 2020;34:1577-1584.